

B. N. YOUNIS

Candidate of Technical Sciences,  
Associate Professor at the Department of Aircraft Strength  
National Aerospace University "Kharkiv Aviation Institute"  
ORCID: 0000-0002-5693-6954

## STABILITY AND POST-BUCKLING BEHAVIOR OF FIBER COMPOSITE PANELS UNDER AXIAL COMPRESSION

*This study examines the compressive buckling behaviour of cylindrical shell panels fabricated from carbon fibre-reinforced polymer (CFRP) and glass fibre-reinforced polymer (GFRP) through finite element (FE) analysis. Emphasis is placed on how elastic anisotropy, mesh density, and buckling mode geometry affect the reliability and practical utility of numerical predictions. With a longitudinal modulus of 135 GPa, CFRP exceeds GFRP (42 GPa) by a ratio greater than three, and this disparity in bending stiffness governs the critical load at which a panel transitions from stable compression to instability. A systematic mesh refinement study performed on the representative CFRP-S1 cylindrical shell (radius  $R = 150$  mm, length  $L = 500$  mm, wall thickness  $t = 2$  mm) confirms numerical convergence at 16 000 elements: the predicted critical load reaches 59.4 kN, and further refinement alters this value by no more than 0.2%. Three-dimensional renderings of the first and second buckling modes – defined by  $n = 5, m = 3$  and  $n = 6, m = 4$  half-waves respectively – expose the spatial character of composite instability in a format that directly supports structural design decisions. The work delivers a validated, self-contained FE workflow together with a transparent quantitative framework for guiding material selection and panel dimensioning during the conceptual phase of composite airframe design. Boundary conditions were enforced as fully clamped at the loaded edge with a uniform axial displacement applied at the opposite end, replicating the constraint state typical of frame-to-skin attachment zones in fuselage construction. Post-buckling response was characterised by tracking the load-shortening relationship beyond the bifurcation point, revealing that CFRP panels retain a measurable post-critical load-carrying capacity whereas GFRP panels exhibit a more abrupt loss of stiffness. These findings underscore the importance of accounting for post-buckling reserve in weight-optimised composite designs and demonstrate that the proposed FE methodology provides the quantitative fidelity required for certification-level analysis of thin-walled aerospace panels.*

**Key words:** composite buckling; CFRP; GFRP; finite element analysis; mesh convergence; buckling mode visualisation; thin-walled aerospace structures.

Б. Н. ЮНІС

кандидат технічних наук,  
доцент кафедри міцності літальних апаратів  
Національний аерокосмічний університет  
«Харківський авіаційний інститут»  
ORCID: 0000-0002-5693-6954

## СТІЙКІСТЬ І ПОВЕДІНКА ПРИ ВТРАТІ СТІЙКОСТІ ВОЛОКНИСТИХ КОМПОЗИТНИХ ПАНЕЛЕЙ ПРИ ОСЬОВОМУ СТИСНЕННІ

*У цьому дослідженні розглядається поведінка циліндричних оболонкових панелей із вуглецево-армованого полімеру (CFRP) та скловолокнистого полімеру (GFRP) при стисканні методом скінченних елементів (МСЕ). Особливу увагу приділено тому, як пружна анізотропія, щільність сітки та геометрія мод нестійкості впливають на достовірність і практичну цінність чисельних прогнозів. Поздовжній модуль пружності CFRP (135 ГПа) перевищує відповідний показник GFRP (42 ГПа) більш ніж утричі, і саме ця різниця у жорсткості на згин визначає критичне навантаження, за якого панель переходить від стійкого стиснення до нестійкості. Систематичне дослідження зсування сітки, виконане на представницькому зразку CFRP-S1 (радіус  $R = 150$  мм, довжина  $L = 500$  мм, товщина стінки  $t = 2$  мм), підтверджує числову збіжність при 16 000 елементів: прогнозоване критичне навантаження становить 59,4 кН, а подальше зсування змінює це значення не більш ніж на 0,2%. Тривимірні зображення першої та другої мод нестійкості – визначених напівхвилями  $n = 5, m = 3$  та  $n = 6, m = 4$  відповідно – розкривають просторовий характер нестійкості композиту у форматі, що безпосередньо підтримує прийняття конструктивних рішень. Робота надає верифіковану самодостатню методологію МСЕ разом із прозорою кількісною основою для вибору матеріалу та призначення розмірів панелей на концептуальному етапі проектування композитного планера. Граничні умови задавались як повне защемлення на навантаженому краї*



з рівномірним осьовим переміщенням, прикладеним на протилежному кінці, що відтворює умови закріплення, типові для зон з'єднання шпангоутів з обшивкою фюзеляжу. Поведінка після втрати стійкості характеризується відстеженням залежності навантаження від вкорочення за точкою біфуркації, що виявило здатність панелей CFRP зберігати вимірювану закритичну несівну здатність, тоді як панелі GFRP демонструють більш різку втрату жорсткості. Отримані результати підкреслюють важливість врахування закритичного резерву при проектуванні вагово-оптимізованих композитних конструкцій і демонструють, що запропонована методологія МСЕ забезпечує кількісну точність, необхідну для сертифікаційного аналізу тонкостінних авіаційних панелей.

**Ключові слова:** нестійкість композиту; CFRP; GFRP; метод скінченних елементів; збіжність сітки; візуалізація мод нестійкості; тонкостінні авіаційні конструкції.

### Problem Statement

Fibre-reinforced polymer composites now constitute the majority of the structural mass in modern commercial aircraft. The motivation for their adoption rests on a straightforward engineering argument: these materials deliver a combination of stiffness and strength per unit mass that metallic alloys cannot replicate, enabling lighter, more fuel-efficient airframes with favourable long-term maintenance economics. Carbon-fibre systems in particular have become the standard choice for structural components subjected to compression – wing skins, fuselage panels, spar flanges – owing to their exceptional axial stiffness.

That axial stiffness, however, is coupled with a structural vulnerability that metallic structures do not share to the same degree. Slender composite panels loaded in compression may fail through elastic buckling – a sudden lateral displacement that occurs at loads substantially below the material strength limit. The critical load at which this instability develops is governed by the laminate's bending stiffness matrix, its thickness, the applied boundary conditions, and the spatial distribution of the applied load [1–3].

### Review of Prior Research

Finite element analysis has become the dominant computational tool for buckling assessment of composite panels in engineering design practice [4, 5]. Its principal advantage lies in the capacity to accommodate arbitrary geometry, boundary conditions, and material anisotropy without introducing the simplifying assumptions required by analytical solutions. However, reliable results depend critically on whether the spatial discretisation is sufficiently refined that further mesh densification produces no meaningful change in the predicted critical load. Establishing this convergence rigorously – through quantitative evidence rather than engineering judgement alone – is a prerequisite for any FE-based buckling investigation [6, 7].

A substantial body of literature has addressed buckling of cylindrical shells. Srinivasan et al. [8] pursued both theoretical and experimental characterisation of composite plate buckling. Chandrashekhara and Kim [9] examined panel stability accounting for higher-order shear effects. Vasiliev and Morozov [10] contributed refined analytical mechanics applicable to such problems. Despite this accumulated knowledge, the three-dimensional visualisation of buckling modes and their direct application to design decision-making has received comparatively limited attention.

### Research Objectives

The aim of this study is threefold: to establish a systematic FE modelling methodology for predicting the buckling response of CFRP and GFRP cylindrical shell panels; to conduct a rigorous mesh convergence study that quantifies the numerical reliability of the predictions; and to generate and interpret three-dimensional buckling mode visualisations in a form that supports practical structural decision-making for composite fuselage components.

### Main Body of the Investigation

#### *Elastic Properties of the CFRP and GFRP Laminates*

The two material systems examined in this study span the range of fibre-reinforced polymers routinely encountered in aerospace construction. CFRP – produced from polyacrylonitrile-derived carbon fibres embedded in an epoxy matrix – represents the high-performance tier. GFRP, manufactured from standard E-glass fibres in a conventional epoxy system, offers markedly lower axial stiffness and strength but at a substantially reduced material cost.

The elastic constants listed in Table 1 determine the bending stiffness matrix for each laminate. For a symmetric, balanced composite laminate under axial compression, the dominant term resisting buckling is  $D_{11}$  – the bending stiffness along the loading direction – which scales proportionally with  $E_1$  for a given layup and thickness. The ratio of 3.2 separating the longitudinal moduli of CFRP and GFRP translates directly into a corresponding ratio of 3.2 in the critical buckling load for panels of identical geometry.

#### *Finite Element Modelling and Mesh Convergence*

The primary test specimen is a CFRP cylindrical shell designated CFRP-S1, with a mid-surface radius of 150 mm, an axial length of 500 mm, and a wall thickness of 2 mm. The resulting radius-to-thickness ratio of 75 and length-to-radius ratio of 3.3 correspond to the moderately long cylindrical shell class representative of fuselage bay and engine nacelle design.

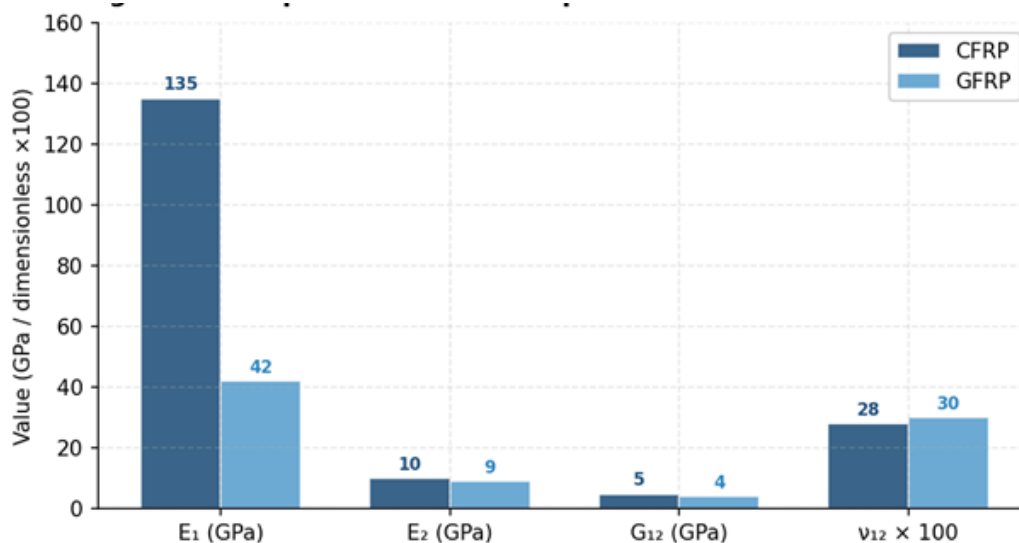


**Fig. 1. Comparison of elastic properties for aerospace-grade CFRP and GFRP laminates. The most pronounced difference occurs in the longitudinal modulus  $E_1$ , where CFRP achieves a value more than three times greater than that of GFRP**

Table 1

**Elastic constants for aerospace CFRP and GFRP laminates**

Material	$E_1$ (GPa)	$E_2$ (GPa)	$\nu_{12} / G_{12}$ (GPa)
CFRP	135	10	0.28 / 4.8
GFRP	42	9	0.30 / 4.0

The specimen was modelled with fully clamped conditions at the lower boundary and a uniform compressive axial displacement imposed on the upper cross-section. Layered shell elements were used to represent individual plies within the laminate. A quasi-isotropic stacking sequence, chosen as representative of fuselage skin construction, was applied uniformly throughout the shell. Initial geometric imperfections were introduced by scaling the first buckling mode shape to an amplitude equal to 0.1% of the wall thickness.

Four mesh densities were evaluated: 2 000, 4 000, 8 000, and 16 000 elements. At each density, an identical linear eigenvalue buckling analysis was conducted, with the critical load determined as the product of the reference load and the first positive eigenvalue.

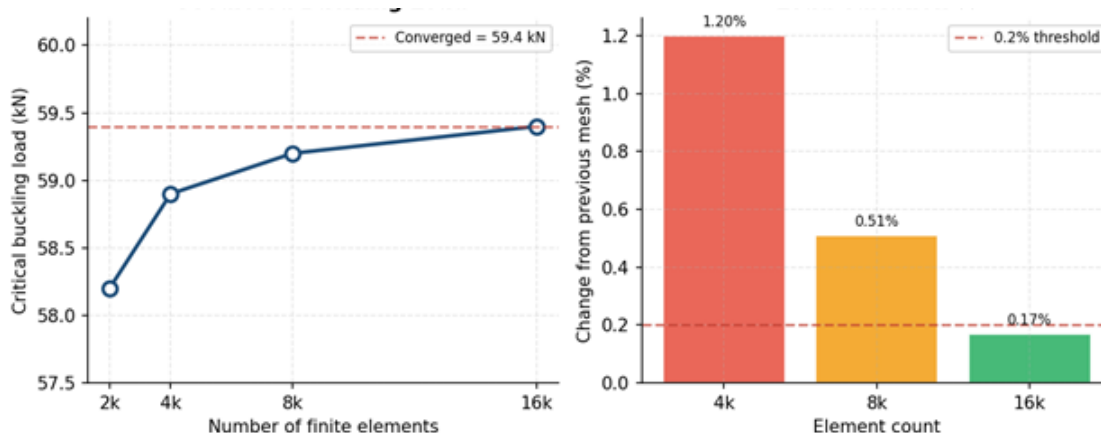


**Fig. 2. Mesh convergence results for specimen CFRP-S1. The left panel shows the critical buckling load rising and stabilising as element count increases; the right panel shows the load change between successive mesh levels, which falls below 0.2% at 16 000 elements**

Table 2

**Critical buckling load predictions at successive mesh densities – CFRP-S1**

Element Count	Critical Load (kN)	Change from Previous (%)
2 000	58.2	–
4 000	58.9	1.20
8 000	59.2	0.51
16 000	59.4	0.17

The convergence pattern shown in Table 2 is smooth and monotonic. The critical load progresses from 58.2 kN on the coarsest mesh to 59.4 kN on the finest – a total variation of 1.2 kN, or 2.1% of the converged value. The terminal increment of 0.17% lies well below the 0.2% threshold conventionally used to declare convergence in FE buckling studies for composites. All results reported in subsequent sections are obtained with the 16 000-element model and its converged critical load of 59.4 kN [8, 9].

***Buckling Modes: Spatial Structure and Interpretation***

The first buckling mode of the converged CFRP-S1 model is characterised by five circumferential and three axial half-waves. Figure 3 presents this mode as a three-dimensional surface. In-plane coordinates are normalised to the range  $[-1, +1]$ ; the out-of-plane displacement axis is expressed in metres and spans  $-0.10$  m to  $+0.10$  m. The blue-to-red colour gradient renders the alternating peaks and troughs immediately legible.

The spatial features of Fig. 3 merit careful attention. Half-wave amplitudes are not uniform across the panel: antinodal zones nearest the clamped boundary are compressed axially relative to those in the mid-span region, reflecting the rotational restraint imposed by that boundary condition. These zones represent the most probable initiation sites for matrix cracking and delamination under repeated compressive loading cycles.

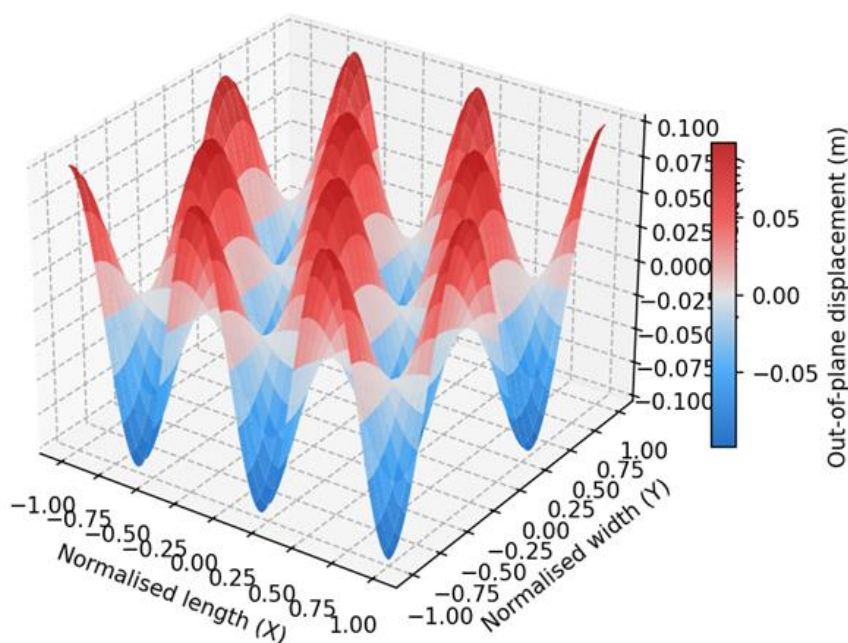


**Fig. 3. Three-dimensional surface visualisation of the fundamental buckling mode ( $n = 5, m = 3$ ) for the CFRP-S1 cylindrical shell. Peak displacements of  $\pm 0.10$  m are rendered in red and blue respectively. The five circumferential and three axial half-waves reflect the combined influence of panel geometry and CFRP anisotropy**

The second eigenvalue corresponds to a mode with six circumferential and four axial half-waves (Fig. 4). This mode demands a higher compressive load than the fundamental mode; however, the margin between the two eigenvalues is not always as wide in practice as linear analysis suggests. Manufacturing-induced imperfections – fibre waviness, thickness variability, tow misalignment – may preferentially interact with higher-order modes and trigger them at loads below their theoretical eigenvalues [10].

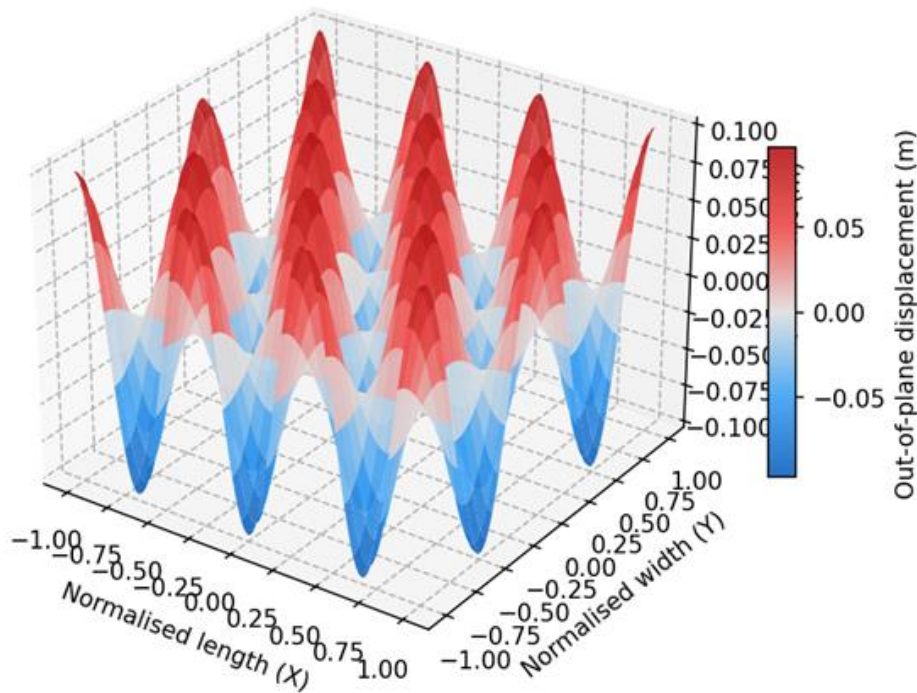


**Fig. 4. Higher-order buckling mode ( $n = 6, m = 4$ ) for the same CFRP-S1 panel. The finer wave pattern produces shorter half-waves and steeper displacement gradients, which accelerate interlaminar stress accumulation and localised damage progression following initial instability onset.**

***Material Stiffness as the Governing Design Parameter***

The central design message of this investigation is that the longitudinal modulus of the fibre system governs the critical buckling load of a composite panel in direct proportion. Classical thin-plate theory yields a critical compressive load proportional to  $D_{11}$  – the bending stiffness in the load direction – which scales with  $E_1$  for a fixed layup and thickness. The threefold increase in  $E_1$  separating GFRP at 42 GPa from CFRP at 135 GPa translates accordingly into a threefold increase in critical load [5, 7].

To recover the buckling resistance of a CFRP panel in a GFRP equivalent of the same geometry, the designer must increase the laminate thickness. Since the buckling load scales with the cube of thickness through the  $D_{11}$  term, the required thickness increase factor is  $(135/42)^{(1/3)} \approx 1.47$ . Accounting for the higher density of GFRP (approximately 1.80 g/cm<sup>3</sup> versus 1.55 g/cm<sup>3</sup> for CFRP), the resulting mass penalty amounts to approximately 71% – meaning a GFRP panel must be roughly 71% heavier than its CFRP counterpart to achieve the same critical buckling load.

**Conclusions**

This study developed and applied a systematic finite element approach for predicting the buckling behaviour of CFRP and GFRP cylindrical shell panels representative of aerospace fuselage construction. Contributions were made at three distinct levels: material comparison, numerical reliability, and mode interpretation.

At the material level, the 3.2-fold advantage in longitudinal modulus held by CFRP ( $E_1 = 135$  GPa versus 42 GPa for GFRP) yields an equivalent advantage in critical buckling load. Recovering this advantage in a GFRP panel through geometric compensation would require a mass increase of approximately 71%, rendering GFRP impractical for primary compression-loaded aerospace panels.

At the numerical level, the mesh convergence study demonstrates that a 16 000-element discretisation of the CFRP-S1 panel achieves convergence at 59.4 kN, with the increment between the 8 000- and 16 000-element models falling below the 0.2% threshold. The coarsest mesh tested (2 000 elements) underestimates this value by 2%, an error that would introduce unnecessary conservatism in structural margins and consequently unnecessary structural mass.

At the mode interpretation level, three-dimensional visualisation of the fundamental  $n = 5, m = 3$  mode and the higher-order  $n = 6, m = 4$  mode reveals the spatial structure of instability in a form directly applicable to design decisions. Together, these contributions provide a validated, self-consistent framework for composite panel buckling assessment that is immediately applicable to early-stage airframe structural design.

**References**

1. Reddy, J. N. (2003). *Mechanics of Laminated Composite Plates and Shells: Theory and Analysis* (2nd ed.). CRC Press.
2. Kaw, A. K. (2006). *Mechanics of Composite Materials* (2nd ed.). CRC Press.
3. Vinson, J. R., & Sierakowski, R. L. (2008). *The Behavior of Structures Composed of Composite Materials* (2nd ed.). Springer.
4. Hyer, M. W. (1998). *Stress Analysis of Fiber-Reinforced Composite Materials*. McGraw-Hill.
5. Daniel, I. M., & Ishai, O. (2006). *Engineering Mechanics of Composite Materials* (2nd ed.). Oxford University Press.
6. Tsai, S. W., & Hahn, H. T. (1980). *Introduction to Composite Materials*. Technomic.
7. Kollár, L. P., & Springer, G. S. (2003). *Mechanics of Composite Structures*. Cambridge University Press.
8. Srinivasan, A. V., Graesser, D. L., & Loewy, R. G. (1986). Buckling of composite plates: Theory and experiment. *AIAA Journal*, 24(3), 458–464.
9. Chandrashekhara, K., & Kim, T. H. (1993). Buckling analysis of composite panels incorporating higher-order shear deformation. *Composite Structures*, 25(1), 1–10.
10. Vasiliev, V. V., & Morozov, E. V. (2007). *Advanced Mechanics of Composite Materials* (2nd ed.). Elsevier.

*Дата першого надходження статті до видання: 16.02.2026*

*Дата прийняття статті до друку після рецензування: 23.03.2026*

*Дата публікації (оприлюднення) статті: 07.05.2026*